HHS Public Access

Author manuscript

Cancer Prev Res (Phila). Author manuscript; available in PMC 2017 May 01.

Published in final edited form as:

Cancer Prev Res (Phila). 2016 May ; 9(5): 406–414. doi:10.1158/1940-6207.CAPR-15-0347.

Inflammation-Related IL-1β/IL-1R Signaling Promotes the Development of Asbestos-Induced Malignant Mesothelioma

Yuwaraj Kadariya[#1], **Craig W. Menges**[#1], **Jacqueline Talarchek**[1], **Kathy Q. Cai**[2], **Andres J. Klein-Szanto**[1,2], **Ralph A. Pietrofesa**[3], **Melpo Christofidou-Solomidou**[3], **Mitchell Cheung**[1], **Brooke T. Mossman**[4], **Arti Shukla**[4], and **Joseph R. Testa**[1]

[1]Cancer Biology Program, Fox Chase Cancer Center, Philadelphia, PA 19111

[2]Histopathology Facility, Fox Chase Cancer Center, Philadelphia, PA 19111

[3]Department of Medicine, Pulmonary, Allergy and Critical Care Division, University of Pennsylvania Perelman School of Medicine, Philadelphia, PA 19104

[4]Department of Pathology, University of Vermont College of Medicine, Burlington, VT, 05405-0068

[#] These authors contributed equally to this work.

Abstract

Exposure to asbestos is causally associated with the development of malignant mesothelioma (MM), a cancer of cells lining the internal body cavities. MM is an aggressive cancer resistant to all current therapies. Once inhaled or ingested, asbestos causes inflammation in and around tissues that come in contact with these carcinogenic fibers. Recent studies suggest that inflammation is a major contributing factor in the development of many types of cancer, including MM. The NALP3/NLRP3 inflammasome, including the component ASC, is thought to be an important mediator of inflammation in cells that sense extracellular insults, such as asbestos, and activates a signaling cascade resulting in release of mature IL-1β and recruitment of inflammatory cells. To determine if inflammasome-mediated inflammation contributes to asbestos-induced MM, we chronically exposed *Asc*-deficient mice and wild-type littermates to asbestos and evaluated differences in tumor incidence and latency. The *Asc*-deficient mice showed significantly delayed tumor onset and reduced MM incidence compared to wild-type animals. We also tested whether inflammation-related release of IL-1β contributes to tumor development in an accelerated mouse model of asbestos-induced MM. $Nf2^{+/-};Cdkn2a^{+/-}$ mice exposed to asbestos in the presence of anakinra, an IL-1 receptor (IL-1R) antagonist, showed a marked delay in the median time of MM onset compared to similarly exposed mice given vehicle control (33.1 weeks versus 22.6 weeks, respectively). Collectively, these studies provide evidence for a link between inflammation-related IL-1β/IL-1R signaling and the development of asbestos-induced MM. Furthermore, these findings provide rationale for chemoprevention strategies targeting IL-1β/IL-1R signaling in high risk, asbestos-exposed populations.

Corresponding Author: Joseph R. Testa, Cancer Biology Program, Fox Chase Cancer Center, Philadelphia, PA 19111. Phone: 215-728-2610; Fax: 215-214-1623; Joseph.Testa@fccc.edu.

Disclosure of Potential Conflicts of Interest: The authors have no potential conflicts of interest to disclose with regard to this work.

Keywords

IL-1β; asbestos; mesothelioma; inflammation; inflammasome; chemoprevention

Introduction

Malignant mesothelioma (MM) is an aggressive cancer that arises primarily from the mesothelial lining of the pleural and peritoneal cavities. Patients with MM usually present with advanced-stage disease that is often surgically inoperable and refractory to standard chemotherapeutic regimens. Epidemiological studies have established that exposure to asbestos fibers is the primary cause of MM (1). Despite asbestos abatement efforts, the incidence of MM in the U.S. has remained stable since 1994, causing ~3,200 deaths annually (2), but will increase by 5-10% per year in Europe over the next 25 years (3). Furthermore, a marked increase in MM incidence is predicted in developing countries, where usage of asbestos is increasing at an alarming rate (4). With estimates of >20 million individuals at risk worldwide, new approaches for the prevention and management of this disease are urgently needed.

MM is a cancer characterized by recurrent genomic losses that typically occur in combination (5). Molecular genetic studies of human MMs have uncovered recurrent somatic mutations of several tumor suppressor genes, particularly *CDKN2A* (encoding p16INK4A and p14ARF) (6, 7), *NF2* (8, 9), and *BAP1* (10, 11). Genetically engineered mouse (GEM) models of MM have demonstrated that haploinsufficiency for *Cdkn2a*, *Nf2* or *Bap1* accelerates asbestos-induced MM onset and progression (12-16), thereby providing both experimental evidence in support of the pivotal role of these tumor suppressor genes in MM pathogenesis and relevant murine models to facilitate preclinical studies of novel chemopreventive and chemotherapeutic agents.

More than a century ago, Virchow demonstrated a link between cancer and inflammation when he observed macrophages and other inflammatory cells in tumor biopsies (17). Upon exposure to asbestos, macrophages are recruited to sites of asbestos deposition, indicating that one physiological response to mineral fiber exposure is inflammation. Mice exposed to asbestos exhibit recruitment of activated macrophages to mesothelium that interacts with asbestos fibers (18). As a result of increased macrophage accumulation, the nearby mesothelial cells are thought to be exposed to pro-inflammatory cytokines such as IL-1β and TNFα (18). Interestingly, IL-1β and TNFα can act in concert with asbestos fibers to transform normal mesothelial cells *in vitro*, suggesting that inflammation may directly contribute to MM development (19, 20). IL-1β, as opposed to TNFα, has been shown to increase the proliferative capacity of mesothelial cells *in vitro* (19, 20). Interestingly, depletion of activated macrophages in an orthotopic mouse model of MM was found to diminish tumorigenesis (21). Collectively, these data imply that recruitment of activated macrophages as a result of inflammation contributes to mesothelial proliferation and transformation through release of the cytokines IL-1β and TNFα.

Macrophages are also thought to directly interact with and phagocytize asbestos fibers (18). Interestingly, it is hypothesized that macrophages and mesothelial cells exposed to asbestos

undergo frustrated phagocytosis of elongated fibers; this process is thought to cause chronic production of reactive oxygen species (ROS) and cytokines, which contribute to transformation of mesothelial cells (22). Thus, chronic inflammation associated with exposure to asbestos may represent a form of extrinsic cancer-related inflammation fundamentally important in MM development, a hypothesis that is addressed herein.

The NALP3/NLRP3 inflammasome is a protein complex made up of NALP3, ASC (apoptosis-associated speck-like protein containing a caspase-associated recruitment domain; designated Asc in the mouse) and caspase-1. The NALP3 inflammasome complex plays an important role in recognizing external stimuli and mediating inflammation in response to certain environmental insults (23-25). Upon activation, the NALP3 inflammasome facilitates the processing of IL-1β from its immature precursor form to a cleaved mature form via caspase-1 mediated activity. The processed IL-1β is then released from macrophages to help stimulate inflammation. The inflammasome is also activated upon exposure to bleomycin and is required for lung inflammation and fibrosis (26). Bleomycin-mediated fibrosis and inflammation can be blocked by an interleukin 1 receptor (IL-1R) antagonist, which suggests that inflammasome-mediated production of mature IL-1β is a required process in the inflammatory response (26).

The NALP3 inflammasome has also been shown to mediate inflammation and IL-1β production from macrophages in response to asbestos and silica (27, 28). Importantly, macrophages deficient for the inflammasome components ASC or NALP3 did not produce increased levels of IL-1β in response to asbestos, suggesting that macrophages produce IL-1β in response to mineral fibers specifically through the NALP3 inflammasome (27). Moreover, macrophages require endocytosis and ROS production for inflammasome activation to occur in response to asbestos. In a model of asbestos inhalation, mice deficient for ASC or NALP3 exhibited reduced inflammatory cell recruitment and decreased cytokine production in the lung (27), suggesting that the NALP3 inflammasome mediates inflammation caused by exposure to asbestos.

In this investigation, we have used *in vivo* approaches with GEM models and a clinically relevant IL-1R antagonist, anakinra, to formally test whether asbestos-induced inflammation is required for MM pathogenesis. We used both an inflammasome-deficient *Asc* knockout model as well as a small molecule inhibitor of IL-1R signaling to test whether a defective inflammasome or pharmacological inhibition of IL-1β/IL-1R signaling could delay MM onset and progression. *Asc*-deficient mice do not mount a pro-inflammatory response to asbestos and silica (27, 28) and, thus, provide an important resource to directly test the importance of asbestos-induced inflammation in MM development/progression. We provide the first *in vivo* evidence with GEM models that inflammation directly contributes to the development of asbestos-induced MM and show that inflammasome-mediated IL-1β/IL-1R signaling contributes to cancer-related inflammation and may represent a promising potential target for the prevention of MM.

Materials and Methods

Experimental animals

Asc-null mice were kindly provided by V.M. Dixit (Genentech) (23). The $Asc^{-/-}$ mice were backcrossed with C57BL/6 mice to generate the various *Asc* genotypes ($^{-/-}$, $^{+/-}$, $^{+/+}$) needed for the asbestos carcinogenicity experiments. $Nf2^{+/-};Cdkn2a^{+/-}$ mice (29) were generated by crossing $Nf2^{+/-}$ and $Cdkn2a^{+/-}$ mice, each backcrossed 6-7 generations into the same FVB background. The $Cdkn2a^{+/-}$ (01XB2, FVB/N.129-$Cdkn2a^{tm1Rdp}$) mice (30), which are haploinsufficient for both p16(Ink4a) and p19(Arf), were obtained from the Mouse Models of Human Cancers Consortium. $Nf2^{+/-}$ mice were obtained from T. Jacks and A.I. McClatchey (31).

Treatment with asbestos

For studies assessing the requirement of inflammation in MM development, $Asc^{-/-}$, $Asc^{+/-}$, and $Asc^{+/+}$ mice were injected intraperitoneally (i.p.) with crocidolite asbestos (UICC grade, SPI Supplies), employing a modified method previously used to induce MM in heterozygous *Tp53* mice (32). Male mice 6 to 8 weeks of age were anesthetized and injected with 400 μg of crocidolite in 500 μl PBS every 21 days for a total of eight injections (total = 3.2 mg) (13, 29). The 21-day interval between injections was selected based on previous work showing that 20 μg to 1 mg of crocidolite injected i.p. stimulates mesothelial cell proliferation for at least 21 days (33). Altogether, 84 animals (26 $^{+/+}$, 29 $^{+/-}$, and 29 $^{-/-}$) were chronically injected with asbestos and closely followed until evidence of disease (see below). Six $Asc^{-/-}$ mice were excluded in the percent disease-free comparisons due to the development of peritonitis in association with the chronic injections of asbestos. Peritonitis was not found in any of the WT or $Asc^{+/-}$ mice.

To investigate the efficacy of an IL-1R antagonist as a chemopreventive agent, $Nf2^{+/-};Cdkn2a^{+/-}$ mice were first weighed at 8-10 weeks of age prior to the start of the experiment. In this experiment, mice were injected i.p. with 800 μg of crocidolite in 500 μl PBS every 21 days for a total of four injections (total = 3.2 mg). Although the total dose of asbestos fibers was identical to that used in the experiments with *Asc*-deficient mice, only four injections of asbestos were used in the studies with $Nf2^{+/-};Cdkn2a^{+/-}$ mice for two reasons: 1) so that the full dose of asbestos could be administered before animals began to show signs of MM, which occurs relatively rapidly in the $Nf2^{+/-};Cdkn2a^{+/-}$ model; and 2) to minimize trauma, as these mice would also receive numerous additional injections of anakinra or placebo. Anakinra (*Kineret*, Amgen), a human recombinant IL-1R antagonist, was dissolved in citrate buffer and diluted to 100 μg/100 μl in citrate buffer. Anakinra was injected i.p. at a concentration of 5 mg/kg body weight (100 μg/injection per adult mouse weighing ~20 gm) 6 hours before the first asbestos injection (23). After each asbestos injection, anakinra was given every third day at the same concentration. In parallel, control $Nf2^{+/-};Cdkn2a^{+/-}$ mice were injected i.p. with 100 μl of citrate buffer. A small gauge needle (21G for asbestos; 26G for anakinra or citrate buffer) and different injection sites were used so that one area of the mouse did not become overly sensitized. Thirty-two $Nf2^{+/-};Cdkn2a^{+/-}$ mice per arm were exposed to asbestos in the presence or absence of the IL-1R antagonist.

Detection of tumors

All *in vivo* studies were performed according to NIH's *Guide for the Care and Use of Laboratory Animals*. The protocol was approved by the Committee on the Ethics of Animal Experiments of the Fox Chase Cancer Center (protocol 00-26). Specifically, all mice were examined daily and sacrificed upon detection of abdominal bloating, weight loss of >10%, labored breathing, severe lethargy, or when tumor burden was otherwise obvious. At that point, mice were euthanized and all internal organs and fluids were collected and sent to our Histopathology Facility for assessment. Detailed analysis of the peritoneal, pleural, and pericardial tissues to detect MM was our highest priority, although complete necropsies were performed on all mice. For the experiment involving *Asc*-deficient mice, we performed ascitic taps on 3 animals from each experimental arm at the beginning of the study in order to develop MM cell lines and to relieve bloating (up to a maximum of three times or until hemorrhagic fluid was observed). Disease onset in animals that received an ascitic tap(s) was considered to be the time of the initial ascitic tap.

Tissue preparation, histology, immunohistochemistry

All organs, including lymph nodes, were collected for examination, and histopathology was carried out with the assistance of the Histopathology Facility of Fox Chase Cancer Center. Tissues were collected and fixed in neutral buffered formalin for 24-48 hours, dehydrated, and then embedded in paraffin. Hematoxylin and eosin (H&E)-stained sections were used for histopathologic evaluation, and unstained sections were used for immunohistochemistry (IHC). Immunohistochemical staining was performed on 5-μm formalin-fixed, paraffin-embedded (FFPE) sections. After deparaffinization and rehydration, FFPE sections were subjected to heat-induced epitope retrieval by steaming in 0.01 M citrate buffer (pH 6.0) for 20 min. After endogenous peroxidase activity was quenched with 3% hydrogen peroxide for 20 min and nonspecific protein binding was blocked with goat serum, sections were incubated overnight with primary monoclonal antibodies.

MMs were diagnosed by two independent pathologists (A.J.K.-S. and K.Q.C.) using standard histopathologic criteria (34). IHC with antibodies specific for various MM-related markers, such as WT1 and mesothelin, was used to differentiate MM from adenocarcinoma. Mice were scored as having MM based on histopathological evidence and if tumor cells exhibited a combination of three or more MM markers, including mesothelin, WT1, E-cadheren and cytokeratin 18/19, as assessed by IHC. The antibodies used are identical to those used in our previous publications on murine MMs (13-15) and are recommended by the commercial vendors for IHC. P-AKT, P-ERK and P-JNK antibodies (Cell Signaling) were used to assess activity of downstream effectors of IL-1β/IL1R signaling.

To assess IHC staining for nuclear Ki67, 2-3 sections from MMs of 6-7 mice per arm were incubated overnight with primary anti-Ki67 monoclonal antibodies (Rat anti-mouse, Dako, 1:100) at 4°C, followed by treatment with biotinylated goat anti-Rat IgG (Dako, 1:200) for 30 min. Detection and visualization of the antibody complexes were carried out using the labeled streptavidin-biotin system (Dako) and chromogen 3,3'-diaminobenzidine, respectively. The slides were then washed, counterstained with hematoxylin, dehydrated with alcohol, cleared in xylene, and mounted. Murine samples that were shown previously to

express high levels of each of the proteins investigated were used as positive controls. As a negative control, the primary antibody was replaced with normal mouse/rabbit IgG to confirm absence of specific staining. For quantitative image analysis, immunostained slides were scanned using an *Aperio* ScanScope CS scanner (Aperio, Vista, CA). Scanned images were then viewed with *Aperio's* image viewer software (ImageScope). Selected regions of interest were outlined manually by a pathologist (K.Q.C.). The proliferative index of individual Ki67-stained tumor sections was quantified using Aperio's Nuclear V9 algorithm.

In vitro anakinra experiments on normal human mesothelial cells

Normal human mesothelial cells (HM3) were purchased from the laboratory of J. Rheinwald (Brigham and Women's Hospital, Harvard Medical School). HM3 cells were starved overnight in LP9-media containing 1% FBS. Cells pre-treated with anakinra or PBS for 3 h were stimulated with recombinant human IL-1β (10 ng/mL; Sigma Aldrich) for 15 min before harvesting and lysing for immunoblot analysis.

Immunoblotting

Immunoblots were prepared with 50 μg of protein/sample, as described (35, 36). Western blot analysis was performed with antibodies against AKT, phospho-AKT (P-AKT), S6 ribosomal protein (S6RP), P-S6RP, JNK, and P-JNK (1:1,000 dilution), all from Cell Signaling, and ERK1/2 and P-ERK1/2 (1:1,000), from Santa Cruz. Appropriate secondary antibodies (anti-rabbit-, anti-mouse- and anti-goat-HRP, all from Santa Cruz) were used at a 1:2,000 dilution.

Evaluation of levels of IL-1β, IL-6 and TNFα in asbestos-exposed *Asc* mice

Asbestos-exposed $Asc^{+/+}$ and $Asc^{+/-}$ mice were analyzed for plasma and peritoneal lavage fluid (PLF) levels of IL-1β, IL-6 and TNFα using ELISA kits purchased from BD Biosciences (BD OptEIA Mouse TNFα and IL-1β ELISA Kits) and R&D systems (mouse IL-6 Quantikine ELISA Kit). For both $Asc^{+/+}$ and $Asc^{+/-}$ mice, blood and PLF samples were collected from 5 mice that were injected 3 days earlier with asbestos, as well as from 5 mice that were not exposed previously. Two independent experiments were performed (total = 40 mice). Immediately following CO_2 euthanization of animals, blood was drawn by heart puncture, collected in sterile tubes containing heparin, and placed on ice. PLF samples were also collected in sterile tubes and initially placed on ice and then frozen at −80°C. Plasma and PLF samples were run undiluted in duplicate and assays were performed according to the manufacturer's instructions. Cytokine levels are reported as picograms per milliliter (pg/ml) of PLF and plasma. Briefly, peritoneal lavage was performed with 5 ml of sterile phosphate-buffered saline (PBS) using an 18-gauge needle.

Statistical analysis

The Fisher exact test was used to assess the statistical significance of differences among experimental groups with respect to time from the initial asbestos injection to obvious signs of asbestos-related disease. The failure time for these analyses was defined as the age at disease detection. The median percent disease-free calculations were determined between asbestos-exposed $Asc^{-/-}$, $Asc^{+/-}$ and $Asc^{+/+}$ mice, as well as between asbestos-exposed

Nf2$^{+/-}$;*Cdkn2a*$^{+/-}$ treated either with IL-1R antagonist (anakinra) or vehicle control. For statistical analysis of MM incidence, a Chi-square test was used. In the experiment with Asc-deficient mice, animals dying before evidence of asbestos-associated disease were omitted from the percent disease-free computations. The excluded animals included 6 *Asc*$^{-/-}$ mice with peritonitis, as well as 3 *Asc*$^{+/-}$ and 2 *Asc*$^{+/+}$ mice for which cause of death could not be determined.

Results

Asbestos-exposed Asc-deficient mice show delayed MM onset, reduced tumor incidence and decreased IL-1β release when compared to asbestos-exposed wild-type mice

Mice with haploinsufficiency or with complete loss of a component (Asc) of the Nalp3 inflammasome, i.e., *Asc*$^{+/-}$ and *Asc*$^{-/-}$ mice, respectively, each showed a statistically significant delay in MM onset, when compared to asbestos-exposed WT (*Asc*$^{+/+}$) littermates. The median percent disease-free, asbestos-exposed *Asc*$^{+/-}$ and *Asc*$^{-/-}$ mice that developed MM was 69.4 and 66.2 weeks, respectively, which was significantly longer than that of asbestos-exposed WT mice (61.6 weeks), as summarized in Figure 1 and Supplemental Figure S1. Additionally, the incidence of MM in *Asc*$^{+/-}$ and *Asc*$^{-/-}$ mice (65% and 55%, respectively) was reduced compared to that of WT mice (80%). The difference in MM incidence was statistically significant between WT mice and *Asc*$^{-/-}$ mice ($p < 0.05$), but not between WT and *Asc*$^{+/-}$ mice (Supplemental Figs. S1 and S2). Note that all tumors that were diagnosed as MM histologically also stained positively for mesothelin and WT1, well-accepted markers for murine MMs. H&E staining and IHC for mesothelin and WT1 in a representative MM from an *Asc*$^{+/-}$ mice are shown in Fig. 2, along with staining for Ki67, the latter indicative of active cellular proliferation in tumor cells. Histologically, most MMs observed were sarcomatoid, *i.e.*, 14 of 21 (67%) from WT mice, 13 of 19 (68%) from *Asc*$^{+/-}$ mice, and 12 of 16 MMs (75%) in *Asc*$^{-/-}$ mice. Most of the remaining MMs were biphasic.

We next assessed the levels of IL-1β, the downstream target of the Asc-inflammasome complex, in the plasma and PLF of WT and *Asc*$^{+/-}$ mice collected 3 days after injection of asbestos or vehicle. As shown in Figure 3A, the relative levels of IL-1β were significantly decreased in plasma from unexposed and asbestos-exposed *Asc*$^{+/-}$ mice when compared to that of corresponding WT animals, consistent with a previous report (37). A similar decrease in IL-1β levels was found in PLF from unexposed and asbestos-exposed *Asc*$^{+/-}$ mice compared to that of WT mice (Fig. 3B). We also evaluated the levels of IL-6 and TNFα, two inflammatory cytokines associated with cancer, in the plasma and PLF of unexposed and asbestos-exposed WT and *Asc*$^{+/-}$ mice. IL-6 levels were significantly downregulated in both the plasma and PLF of unexposed and asbestos-injected *Asc*$^{+/-}$ mice when compared to corresponding WT animals (Fig. 3A and B). The levels of TNFα were not significantly different in the plasma and PLF of unexposed WT and *Asc*$^{+/-}$ mice; however, they were lower in both plasma and PLF of asbestos-exposed *Asc*$^{+/-}$ mice compared to WT controls (Fig. 3A and B). Together, these data demonstrate a decrease in inflammatory cytokine release in unexposed and asbestos-exposed *Asc*-deficient mice compared to WT mice, consistent with a central role of the inflammasome in asbestos-mediated inflammation.

The IL-1β receptor antagonist anakinra delays asbestos-induced tumorigenesis in an accelerated mouse model of MM

We next addressed whether IL-1β release mediated by the inflammasome could be targeted as a chemoprevention strategy for asbestos-induced MM. We used a *Nf2*$^{+/-}$;*Cdkn2a*$^{+/-}$ double knockout mouse model, which we previously reported develop MM in an accelerated manner upon exposure to asbestos, *i.e.*, ~23 weeks in *Nf2*$^{+/-}$;*Cdkn2a*$^{+/-}$ mice versus 52 weeks in WT littermates (29). Thus, this accelerated model has advantages for more rapid assessment of chemoprevention agents. Male *Nf2*$^{+/-}$;*Cdkn2a*$^{+/-}$ mice were chronically exposed to asbestos in the presence or absence of the IL-1R antagonist anakinra, and median percent disease-free animals and tumor development was assessed. All mice in both experimental arms eventually developed MM, although onset of disease symptoms was significantly delayed in the anakinra-treated animals. As shown in Figure 4A, *Nf2*$^{+/-}$;*Cdkn2a*$^{+/-}$ mice treated with anakinra had an approximately 50% longer median percent disease-free rate (33.1 weeks) than in vehicle-treated mice (22.6 weeks). MMs from mice treated with anakinra showed decreased IHC staining for Ki67 when compared to MMs from vehicle-treated mice (Fig. 4B, C), suggesting that the delayed onset of tumors observed in anakinra-treated animals is mechanistically due, at least in part, to inhibited proliferation of transformed MM cells. We observed no obvious difference between anakinra-treated and placebo-treated animals with regard to the number of macrophage recruited in MMs from these animals.

To identify pathways downstream of IL-1β /IL-1R signaling that are inhibited by anakinra in mesothelial cells, *in vitro* studies were performed with HM3 human mesothelial cells. The cells were serum starved overnight and then stimulated with IL-1β in the presence or absence of anakinra. Cells were harvested 15 min after stimulation with IL-1β, and protein extracts were analyzed by immunoblotting. Pathways selected for analysis were those known to be regulated by IL-1β and potentially important in MM pathogenesis. To this end, we found that anakinra was able to block IL-1β-stimulated activation of AKT, MAPK-ERK, mTOR-S6RP and JNK signaling pathways (Fig. 5A). Concordantly, MMs from anakinra-treated *Nf2*$^{+/-}$;*Cdkn2a*$^{+/-}$ mice showed decreased IHC staining for phosphorylated P-AKT, P-ERK and P-JNK, when compared to that of MMs arising in vehicle-treated control mice (Fig. 5B). Together, these findings suggest that asbestos exposure leads to IL-1β/IL-1R signaling that contributes to MM cell proliferation and downstream oncogenic signaling, and that inhibition of IL-1β/IL-1R signaling with an IL-1R antagonist can delay MM tumorigenesis.

Discussion

The role of inflammation in cancer pathogenesis is an exciting, growing field, with many solid tumors of various origins being influenced by the tumor microenvironment and cells of the immune system. Exposure to asbestos fibers, both in humans and animal models, causes an inflammatory response primarily mediated by macrophages that attempt to phagocytize these fibers in and around the mesothelial lining. Hillegass et al. have shown that human mesothelial cells also have inflammasomes and can perpetuate inflammation in the absence of immune cells (38).

With longer pathogenic fibers, “frustrated” phagocytosis has been hypothesized to cause mesothelial cell proliferation due to the release of cytokines such as IL-1β and TNF-α (22). Moreover, the NALP3 inflammasome is now known to mediate inflammation and the release of mature IL-1β from macrophages in response to asbestos and silica to cause local inflammation (27, 28). Similarly, asbestos and erionite fibers are able to prime and activate the NALP3 inflammasome, which triggers an autocrine feedback loop modulated via the IL-1R in mesothelial cells targeted in pleural infection, fibrosis, and carcinogenesis (38). Thus, the inflammation caused by exposure to asbestos requires the inflammasome, and targeting this pathway would be expected to prevent or diminish inflammation and delay tumor development.

In this report, we have formally tested whether inflammasome-mediated inflammation is required for asbestos-induced MM development. Our findings indicate that deficiency for the inflammasome component *Asc* is not sufficient to prevent asbestos-induced MM development, although a decrease in MM incidence and a significantly longer tumor latency was observed in $Asc^{-/-}$ mice when compared to similarly exposed WT littermates (Supplemental Figs. S1 and S2). While a statistically significant difference in median percent disease-free animals was observed between WT and $Asc^{+/-}$ mice, the difference in MM frequency was not (Figs. 1 and S2), indicating that haploinsufficiency for *Asc* is, as expected, less effective than total loss of *Asc* with regard to asbestos-induced MM incidence.

We did not observe a statistically significant difference in the median percent disease-free animals between asbestos-exposed $Asc^{+/-}$ and $Asc^{-/-}$ mice. However, this finding was complicated by the fact that six $Asc^{-/-}$ mice had to be euthanized due to peritonitis, which was confirmed by cytological assessment of peritoneal fluid. While the infected $Asc^{-/-}$ animals were omitted in the tumor onset and percent disease-free calculations, it is noteworthy that none of the $Asc^{+/-}$ or WT mice showed any evidence of infection. Thus, the findings suggest that the immune system of $Asc^{-/-}$ mice was compromised, which likely played a role in their overall health and survival. This is consistent with other studies that have shown that inflammasome-deficient mice are predisposed to infection due to a weakened inflammatory response (39).

We demonstrated that at 3 days post-asbestos exposure, IL-1β levels were markedly lower in plasma and PLF of asbestos-exposed $Asc^{+/-}$ mice compared to that of WT animals (Fig. 3A, B). Interestingly, however, at 3 months post-exposure, there was no detectable difference in the levels of IL-1β in the serum or PLF of asbestos-exposed mice of any genotype tested (data not shown). A previous study also showed that upregulation of IL-1β by the inflammasome in asbestos-exposed mice usually subsided by day 9 post-exposure (37). We surmise that although inflammasome-mediated IL-1β release contributes to MM onset, it may not be required for maintenance of the tumor. IL-6 and TNFα, two inflammatory cytokines linked to cancer, were also found to be downregulated in *Asc*-deficient mice compared to WT control mice, suggesting that overall inflammation due to asbestos exposure is dampened in these animals (Fig. 3A and B). Interestingly, IL-1β has been previously shown to regulate IL-6 and TNFα via different mechanisms, perhaps explaining why both were downregulated in asbestos-exposed $Asc^{+/-}$ mice (40, 41).

Although the experiments with *Asc*-deficient mice implicated IL-1β-mediated inflammation in MM pathogenesis, we wanted to determine if targeting this pathway could be exploited as a chemoprevention strategy in asbestos-exposed mice. To this end, we demonstrated that the IL-1R antagonist anakinra could delay asbestos-induced tumor formation in an accelerated mouse model of MM. Treatment of mice with anakinra during and post-asbestos exposure delayed time of death due to MM by about 50% (Fig. 4A). Additionally, the proliferative capacity of MMs from anakinra-treated mice was markedly decreased when compared to MMs from vehicle-treated mice (Fig. 4B). These data suggest that IL-1β signaling contributes to the proliferative capacity of tumors in asbestos-exposed mice. We further demonstrated, both *in vitro* and *in vivo*, that anakinra is capable of blocking oncogenic signaling nodes downstream of the IL-1R (Fig. 5A and B), which have previously been shown to be important to MM cell proliferation, survival and invasiveness. However, as noted above, all anakinra-treated mice eventually developed MM, although with a prolonged latency compared to vehicle-treated mice. Thus, we presume that other cytokines or immune components of the microenvironment also play a significant role(s) in MM pathogenesis and can compensate for diminished IL-1β signaling resulting from treatment with anakinra. Drawing parallels to the human disease counterpart, these data demonstrate in a preclinical proof-of-principle model that high-risk individuals chronically exposed to asbestos or other carcinogenic mineral fibers such as erionite might benefit from chemoprevention strategies targeting inflammation-related IL1-β/IL-1R signaling.

These data are the first to our knowledge directly linking asbestos and IL-1β signaling to MM pathogenesis in GEM models of the disease. While the pharmacological evidence from the studies with anakinra provides a strong link between inflammation-related IL-1β/IL-1R signaling and MM development, the genetic evidence generated by studies with *Asc*-deficient mice are less striking. Although *Asc*-deficient mice exhibited a statistically significant delay in tumor onset, the mice showed a relatively modest decrease in overall incidence of MM. A study performed by Australian investigators showed that although IL-1β release was diminished in inflammasome-deficient mice, MM tumor incidence did not differ significantly between inflammasome-deficient *NLRP3*−/− mice (BALB/c background) and WT controls (37). Asbestos (3.0 mg/mouse, similar to the 3.2 mg/mouse used in our experiments), was given as a single bolus injection in that investigation, whereas we used serial injections of lower doses of asbestos given over ~5 months. A single bolus injection of a large quantity of asbestos into the peritoneum of mice often results in large granulomas and a low incidence and longer latency of MM (42). Thus, we chose to administer eight injections of 400 μg of crocidolite in $Asc^{+/-}$ mice, given every 3 weeks, in an attempt to induce a repeated state of inflammation, which has been shown to faithfully cause MM in mice of various backgrounds and genotypes (12-15, 32). In addition to differences in the injection protocols used in the two studies, another difference in the studies is that Chow *et al.* (37) used *Nlrp3*-deficient mice, while we used *Asc*-deficient mice. Significantly, our conclusions about the importance of inflammasome-related IL-1β/IL-1R signaling are bolstered by our anakinra administration studies.

In conclusion, this report provides experimental evidence implicating inflammation in a cancer whose etiology is connected with environmental exposure to a known carcinogen: asbestos. Our findings indicate that the inflammasome contributes to asbestos-induced MM

development, in part through the production and release of IL-1β to promote mesothelial cell proliferation and transformation into a deadly cancer, MM. Additionally, the findings of our studies with anakinra provide rationale for targeting inflammation and IL-1β/IL-1R signaling as a potential chemoprevention strategy for cohorts chronically exposed to asbestos or other carcinogenic mineral fibers.

Supplementary Material

Refer to Web version on PubMed Central for supplementary material.

Acknowledgments

Financial Support: This work was supported by DOD Grant W81XWH-10-1-0462, an appropriation from the Commonwealth of Pennsylvania, a gift from the Local #14 Mesothelioma Fund of the International Association of Heat and Frost Insulators & Allied Workers in memory of Hank Vaughan and Alice Haas (J.R. Testa), and by NIH grants R01 ES021110 (A. Shukla), P42 ES023720, UPenn Superfund Research and Training Program Center (J.R. Testa and M. Christofidou-Solomidou), and CA06927 (Fox Chase Cancer Center).

References

1. Wagner JC, Slegga CA, Marchand P. Diffuse pleural mesothelioma and asbestos exposure in the North Western Cape Province. Br J Ind Med. 1960; 17:260–71. [PubMed: 13782506]
2. Henley SJ, Larson TC, Wu M, Antao VC, Lewis M, Pinheiro GA, et al. Mesothelioma incidence in 50 states and the District of Columbia, United States, 2003-2008. Int J Occup Environ Health. 2013; 19:1–10. [PubMed: 23582609]
3. Goldberg M, Imbernon E, Rolland P, Gilg Soit Ilg A, Savès M, de Quillacq A, et al. The French National Mesothelioma Surveillance Program. Occup Environ Med. 2006; 63:390–5. [PubMed: 16469823]
4. Burki T. Health experts concerned over India's asbestos industry. Lancet. 2010; 375:626–7. [PubMed: 20198723]
5. Flejter WL, Li FP, Antman KH, Testa JR. Recurring loss involving chromosomes 1, 3, and 22 in malignant mesothelioma: possible sites of tumor suppressor genes. Genes, Chromosomes Cancer. 1989; 1:148–54. [PubMed: 2487155]
6. Cheng JQ, Jhanwar SC, Klein WM, Bell DW, Lee W-C, Altomare DA, et al. *p16* alterations and deletion mapping of 9p21-p22 in malignant mesothelioma. Cancer Res. 1994; 54:5547–51. [PubMed: 7923195]
7. Xio S, Li D, Vijg J, Sugarbaker DJ, Corson JM, Fletcher JA. Codeletion of p15 and p16 in primary malignant mesothelioma. Oncogene. 1995; 11:511–5. [PubMed: 7630635]
8. Bianchi AB, Mitsunaga S-I, Cheng JQ, Klein WM, Jhanwar SC, Seizinger B, et al. High frequency of inactivating mutations in the neurofibromatosis type 2 gene (*NF2*) in primary malignant mesotheliomas. Proc Natl Acad Sci U S A. 1995; 92:10854–8. [PubMed: 7479897]
9. Sekido Y, Pass HI, Bader S, Mew DJY, Christman MF, Gazdar AF, et al. Neurofibromatosis type 2 (*NF2*) gene is somatically mutated in mesothelioma but not in lung cancer. Cancer Res. 1995; 55:1227–31. [PubMed: 7882313]
10. Bott M, Brevet M, Taylor BS, Shimizu S, Ito T, Wang L, et al. The nuclear deubiquitinase BAP1 is commonly inactivated by somatic mutations and 3p21.1 losses in malignant pleural mesothelioma. Nat Genet. 2011; 43:668–72. [PubMed: 21642991]
11. Testa JR, Cheung M, Pei J, Below JE, Tan Y, Sementino E, et al. Germline BAP1 mutations predispose to malignant mesothelioma. Nat Genet. 2011; 43:1022–5. [PubMed: 21874000]
12. Altomare DA, Vaslet CA, Skele KL, De Rienzo A, Devarajan K, Jhanwar SC, et al. A mouse model recapitulating molecular features of human mesothelioma. Cancer Res. 2005; 65:8090–5. [PubMed: 16166281]

13. Altomare DA, Menges CW, Pei J, Zhang L, Skele-Stump KL, Carbone M, et al. Activated TNF-alpha/NF-kappaB signaling via down-regulation of Fas-associated factor 1 in asbestos-induced mesotheliomas from Arf knockout mice. Proc Natl Acad Sci U S A. 2009; 106:3430–5.
14. Altomare DA, Menges CW, Xu J, Pei J, Zhang L, Tadevosyan A, et al. Losses of both products of the Cdkn2a/Arf locus contribute to asbestos-induced mesothelioma development and cooperate to accelerate tumorigenesis. PLoS One. 2011; 6:e18828. [PubMed: 21526190]
15. Xu J, Kadariya Y, Cheung M, Pei J, Talarchek J, Sementino E, et al. Germline mutation of Bap1 accelerates development of asbestos-induced malignant mesothelioma. Cancer Res. 2014; 74:4388–97. [PubMed: 24928783]
16. Napolitano A, Pellegrini L, Dey A, Larson D, Tanji M, Flores EG, et al. Minimal asbestos exposure in germline BAP1 heterozygous mice is associated with deregulated inflammatory response and increased risk of mesothelioma. Oncogene. Jun 29.2015 [Epub ahead of print].
17. Srikrishna G, Freeze HH. Endogenous damage-associated molecular pattern molecules at the crossroads of inflammation and cancer. Neoplasia. 2009; 11:615–28. [PubMed: 19568407]
18. Bielefeldt-Ohmann H, Fitzpatrick DR, Marzo AL, Jarnicki AG, Himbeck RP, Davis MR, et al. Patho- and immunobiology of malignant mesothelioma: characterisation of tumour infiltrating leucocytes and cytokine production in a murine model. Cancer Immunol Immunother. 1994; 39:347–59. [PubMed: 8001022]
19. Stadlmann S, Pollheimer J, Renner K, Zeimet AG, Offner FA, Amberger A. Response of human peritoneal mesothelial cells to inflammatory injury is regulated by interleukin-1beta and tumor necrosis factor-alpha. Wound Repair Regen. 2006; 14:187–94. [PubMed: 16630108]
20. Wang Y, Faux SP, Hallden G, Kirn DH, Houghton CE, Lemoine NR, et al. Interleukin-1beta and tumour necrosis factor-alpha promote the transformation of human immortalised mesothelial cells by erionite. Int J Oncol. 2004; 25:173–8. [PubMed: 15202003]
21. Miselis NR, Wu ZJ, Van Rooijen N, Kane AB. Targeting tumor-associated macrophages in an orthotopic murine model of diffuse malignant mesothelioma. Mol Cancer Ther. 2008; 7:788–99. [PubMed: 18375821]
22. Ramos-Nino ME, Testa JR, Altomare DA, Pass HI, Carbone M, Bocchetta M, et al. Cellular and molecular parameters of mesothelioma. J Cell Biochem. 2006; 98:723–34. [PubMed: 16795078]
23. Mariathasan S, Newton K, Monack DM, Vucic D, French DM, Lee WP, et al. Differential activation of the inflammasome by caspase-1 adaptors ASC and Ipaf. Nature. 2004; 430:213–8. [PubMed: 15190255]
24. Pedra JH, Cassel SL, Sutterwala FS. Sensing pathogens and danger signals by the inflammasome. Curr Opin Immunol. 2009; 21:10–6. [PubMed: 19223160]
25. Willingham SB, Bergstralh DT, O'Connor W, Morrison AC, Taxman DJ, Duncan JA, et al. Microbial pathogen-induced necrotic cell death mediated by the inflammasome components CIAS1/cryopyrin/NLRP3 and ASC. Cell Host Microbe. 2007; 2:147–59. [PubMed: 18005730]
26. Gasse P, Mary C, Guenon I, Noulin N, Charron S, Schnyder-Candrian S, et al. IL-1R1/MyD88 signaling and the inflammasome are essential in pulmonary inflammation and fibrosis in mice. J Clin Invest. 2007; 117:3786–99. [PubMed: 17992263]
27. Dostert C, Petrilli V, Van Bruggen R, Steele C, Mossman BT, Tschopp J. Innate immune activation through Nalp3 inflammasome sensing of asbestos and silica. Science. 2008; 320:674–7. [PubMed: 18403674]
28. Cassel SL, Eisenbarth SC, Iyer SS, Sadler JJ, Colegio OR, Tephly LA, et al. The Nalp3 inflammasome is essential for the development of silicosis. Proc Natl Acad Sci U S A. 2008; 105:9035–40. [PubMed: 18577586]
29. Menges CW, Kadariya Y, Altomare D, Talarchek J, Neumann-Domer E, Wu Y, et al. Tumor suppressor alterations cooperate to drive aggressive mesotheliomas with enriched cancer stem cells via a p53-miR34a-c-Met axis. Cancer Res. 2014; 74:1261–71. [PubMed: 24371224]
30. Serrano M, Lee H-W, Chin L, Cordon-Cardo C, Beach D, DePinho RA. Role of the *INK4a* locus in tumor suppression and cell mortality. Cell. 1996; 85:27–37. [PubMed: 8620534]
31. McClatchey AI, Saotome I, Mercer K, Crowley D, Gusella JF, Bronson RT, et al. Mice heterozygous for a mutation at the *Nf2* tumor suppressor locus develop a range of highly metastatic tumors. Genes Dev. 1998; 12:1121–33. [PubMed: 9553042]

32. Marsella JM, Liu BL, Vaslet CA, Kane AB. Susceptibility of *p53*-deficient mice to induction of mesothelioma by crocidolite asbestos fibers. Environ Health Perspect. 1997; 105:1069–72. [PubMed: 9400702]
33. Macdonald JL, Kane AB. Mesothelial cell proliferation and biopersistence of wollastonite and crocidolite asbestos fibers. Fund Appl Toxicol. 1997; 38:173–83.
34. Davis JM, Dungworth DL, Boorman GA. Concordance in diagnosis of mesotheliomas. Toxicol Path. 1996; 24:662–3. [PubMed: 8923695]
35. Xiao G, Gallagher R, Shetler J, Skele K, Altomare D, Pestell R, et al. The NF2 tumor suppressor gene product, merlin, inhibits cell proliferation and cell cycle progression by repressing cyclin D1 expression. Mol Cell Biol. 2005; 25:2384–94. [PubMed: 15743831]
36. Menges CW, Chen Y, Mossman BT, Chernoff J, Yeung AT, Testa JR. A phosphotyrosine proteomic screen identifies multiple tyrosine kinase signaling pathways aberrantly activated in malignant mesothelioma. Genes Cancer. 2010; 1:493–505. [PubMed: 20672017]
37. Chow MT, Tschopp J, Möller A, Smyth MJ. NLRP3 promotes inflammation-induced skin cancer but is dispensable for asbestos-induced mesothelioma. Immunol Cell Biol. 2012; 90:983–6. [PubMed: 23010873]
38. Hillegass JM, Miller JM, MacPherson MB, Westbom CM, Sayan M, Thompson JK, et al. Asbestos and erionite prime and activate the NLRP3 inflammasome that stimulates autocrine cytokine release in human mesothelial cells. Part Fibre Toxicol. 2013; 10:39. [PubMed: 23937860]
39. Benko S, Philpott DJ, Girardin SE. The microbial and danger signals that activate Nod-like receptors. Cytokine. 2008; 43:368–73. [PubMed: 18715799]
40. Bethea JR, Chung IY, Sparacio SM, Gillespie GY, Benveniste EN. Interleukin-1 beta induction of tumor necrosis factor-alpha gene expression in human astroglioma cells. J Neuroimmunol. 1992; 36:179–91. [PubMed: 1732280]
41. Cahill CM, Rogers JT. Interleukin (IL) 1beta induction of IL-6 is mediated by a novel phosphatidylinositol 3-kinase-dependent AKT/IkappaB kinase alpha pathway targeting activator protein-1. J Biol Chem. 2008; 283:25900–12. [PubMed: 18515365]
42. Moalli PA, MacDonald JL, Goodglick LA, Kane AB. Acute injury and regeneration of the mesothelium in response to asbestos fibers. Am J Pathol. 1987; 128:426–45. [PubMed: 2820232]

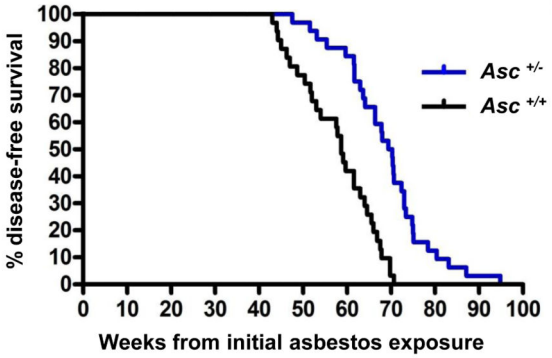

	Asc +/+	Asc +/-	Significance
Median survival (wks)	61.6	69.4	p < 0.0001
Mesothelioma	21/26 (80%)	19/29 (65%)	p < 0.2

Figure 1.

Asc-deficiency significantly delays malignant mesothelioma (MM) development in mice chronically exposed to asbestos. *Top,* Kaplan-Meier curves of percent disease-free animals demonstrate increased latency of asbestos-induced MM in heterozygous *Asc* ($Asc^{+/-}$) mice than in asbestos-treated wild-type (WT, $Asc^{+/+}$) littermates. *Bottom,* summary of differences in median percent disease-free animals and MM incidence in $Asc^{+/-}$ and WT mice. Note that the difference in the percentage of disease-free animals, but not MM incidence, between WT and $Asc^{+/-}$ mice was highly significant ($p < 0.0001$). However, the difference in MM incidence between WT and homozygous $Asc^{-/-}$ mice was statistically significant ($p < 0.05$) (see Supplemental Figs. S1 and S2).

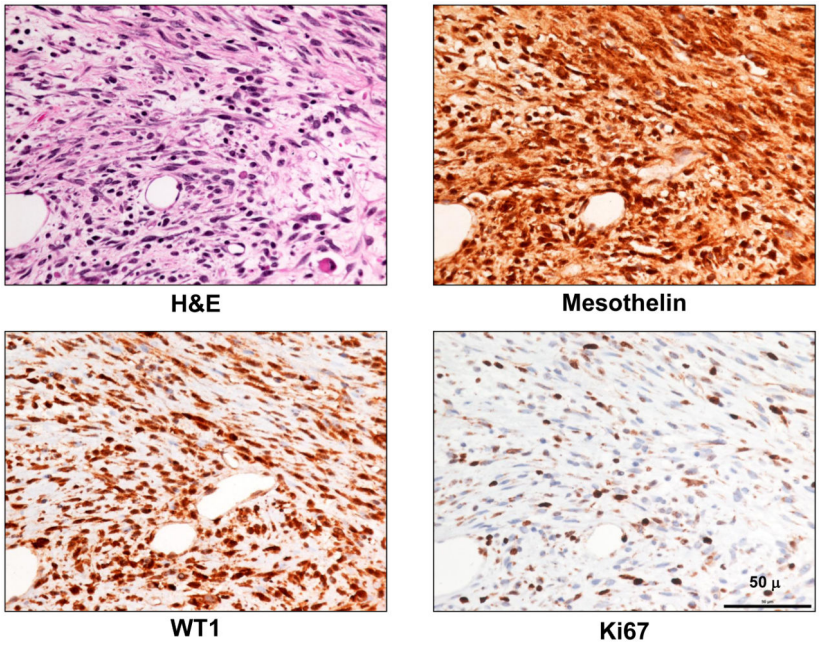

Figure 2.

Histopathologic assessment of MM in an *Asc*$^{+/-}$ mouse. Serial tumor sections depicting H&E staining (*top left panel*) and IHC for MM markers mesothelin (*top right*) and WT1 (*bottom left*) in a representative MM from an *Asc*$^{+/-}$ mouse; Ki67 staining (*lower right*) indicates active cellular proliferation in the MM cells. All original images are at 400X magnification. Scale bar = 50 µ.

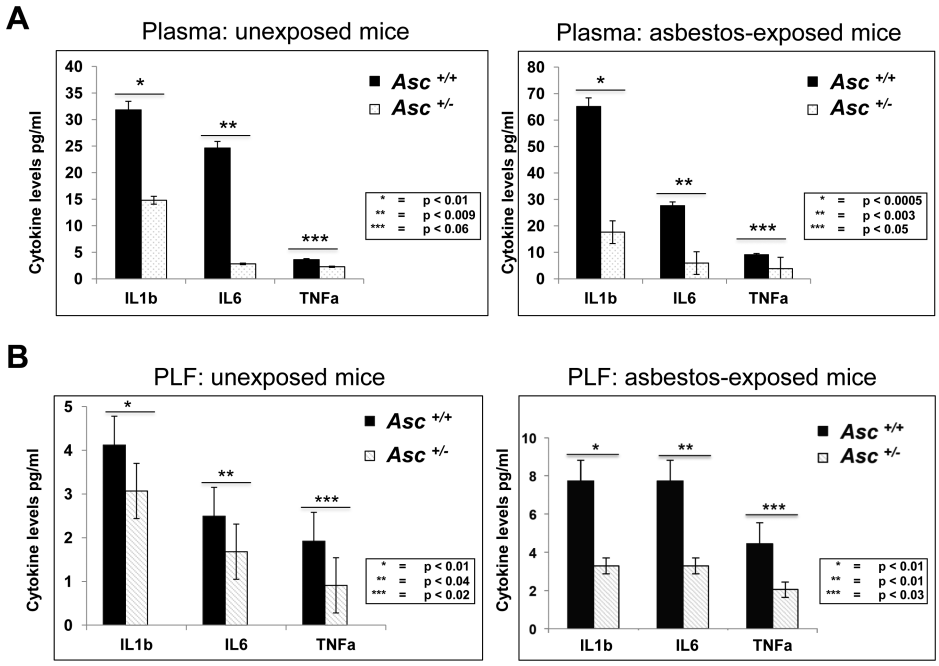

Figure 3.

Decreased levels of IL-1β and other inflammatory cytokines in serum and peritoneal lavage fluid (PLF) from *Asc*$^{+/-}$ mice compared to that of WT (*Asc*$^{+/+}$) mice. **A)** IL-1β, IL-6 and TNFα levels in serum of *Asc*$^{+/-}$ and *Asc* $^{+/+}$ mice exposed or not (unexposed) to asbestos. **B)** IL-1β, IL-6 and TNFα levels in PLF of *Asc*$^{+/-}$ and *Asc* $^{+/+}$ mice exposed or unexposed to asbestos. P-values for differences between the indicated samples from *Asc*$^{+/+}$ (black bars) and *Asc*$^{+/-}$ (white bars) mice are provided for each cytokine and experimental condition tested.

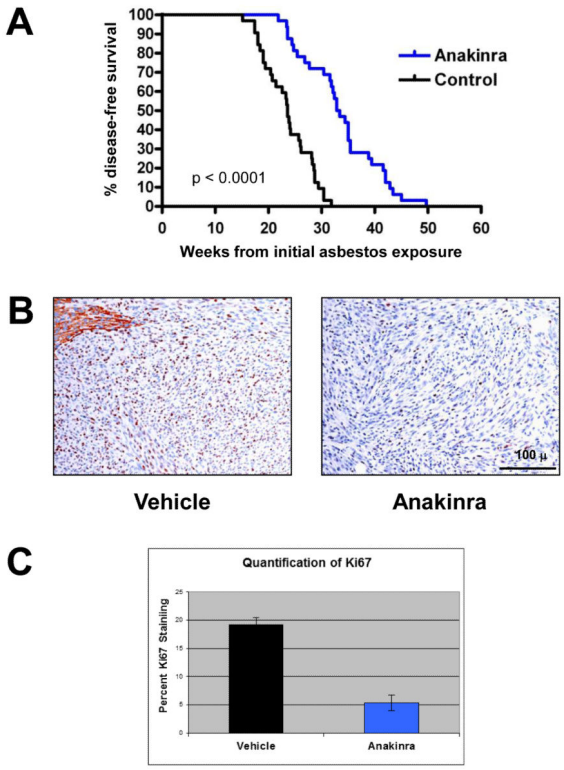

Figure 4.

Anakinra treatment delays tumor onset and inhibits cell proliferation in a mouse model of accelerated asbestos-induced MM. **A)** Kaplan-Meier curves of asbestos-exposed *Nf2*$^{+/-}$;*Cdkn2a*$^{+/-}$ mice treated with anakinra or vehicle (citrate buffer). Treatment of asbestos-exposed *Nf2*$^{+/-}$;*Cdkn2a*$^{+/-}$ mice with anakinra resulted in significantly prolonged survival compared to that observed in vehicle-treated littermates. **B)** Ki67 nuclear staining (brown) of MMs from vehicle- and anakinra-treated mice. Note that adjacent normal liver in vehicle-treated mouse (upper left) shows non-specific cytoplasmic staining. Original images: 200X magnification. Representative 100-μm scale bar is shown. **C)** Quantification of the average percentage of Ki67-positive nuclei in MM tumors from mice treated with anakinra or vehicle. Error bars represent standard deviation of multiple tumor sections from 6-7 mice per arm.

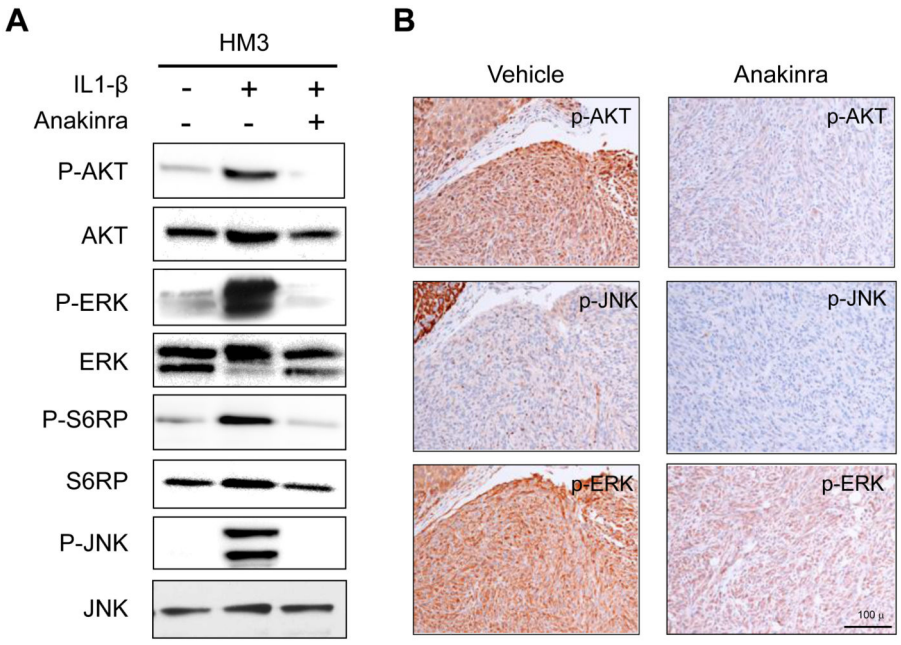

Figure 5.

Anakinra inhibits IL-1β/IL-1R signaling both *in* vitro and *in vivo.* **A)** Immunoblot analysis of normal human mesothelial cells (HM3) starved overnight and then stimulated with IL-1β in the presence or absence of anakinra. Anakinra-treated cells show markedly decreased activity of AKT, ERK and JNK, as illustrated by decreased expression using phospho (P)-specific antibodies. **B)** Immunohistochemical staining (reddish brown) for P-AKT, P-JNK and P-ERK in MMs derived from asbestos-exposed mice treated or not with anakinra. Original images: 200X magnification. Scale bar = 100 µ.